Supporting Information

Effect of the biphenyl neolignan honokiol on $A\beta_{42}$-induced toxicity in *Caenorhabditis elegans*, $A\beta_{42}$ fibrillation, cholinesterase activity, DPPH radicals, and iron(II) chelation

Srinivas Kantham,[‡] Stephen Chan,[‡] Gawain McColl,[§] Jared A. Miles,[‡] Suresh Kumar Veliyath,[‡] Girdhar Singh Deora,[‡] Satish N. Dighe,[‡] Samira Khabbazi,[‡] Marie-Odile Parat[‡] and Benjamin P. Ross*[,‡]

[‡]*School of Pharmacy, The University of Queensland, Brisbane, Queensland 4072, Australia.*

[§]*The Florey Institute of Neuroscience and Mental Health, University of Melbourne, Victoria 3010, Australia.*

*Corresponding author

E-mail: b.ross1@uq.edu.au (B.P. Ross)

Tel.: +61 7 33461900; fax: +61 7 33461999.

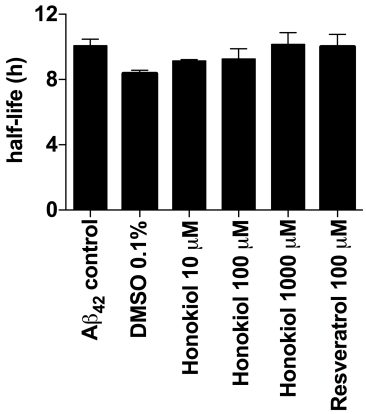

Figure S1. Half-life of $A\beta_{42}$ fibrillation monitored by *in situ* ThT fluorescence. $A\beta_{42}$ (27 μM) was incubated with honokiol (10, 100, and 1000 μM), resveratrol (100 μM), or EGCG (100 μM) in phosphate buffer (20 mM, pH 7.4, *I* 0.17 M, containing 20 μM ThT) at 37˚C under quiescent conditions. Honokiol and resveratrol samples contained DMSO (0.1% v/v). Values are the mean + SEM of three independent experiments. Statistical significance was determined by one-way ANOVA followed by Tukey's multiple comparisons test with no significant differences found between groups. EGCG prevented the formation of a sigmoidal kinetic growth curve hence no half-life value was recorded.

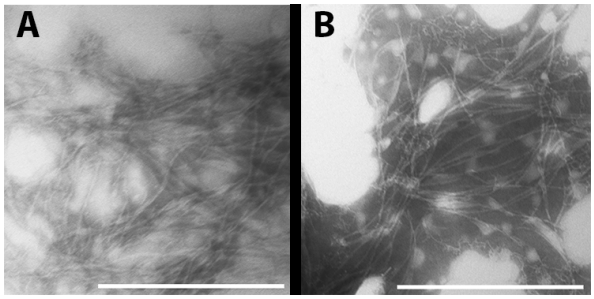

Figure S2. TEM images showing the morphology of $A\beta_{42}$ aggregates in the presence of 0.1% v/v DMSO. $A\beta_{42}$ (27 μM) was incubated in phosphate buffer (20 mM, pH 7.4, I 0.17 M) at 37˚C under quiescent conditions. TEM images of: (A) $A\beta_{42}$ + DMSO (0.1 % v/v) control on day 1; (B) $A\beta_{42}$ + DMSO (0.1 % v/v) control on day 7. The scale bar represents 500 nm.

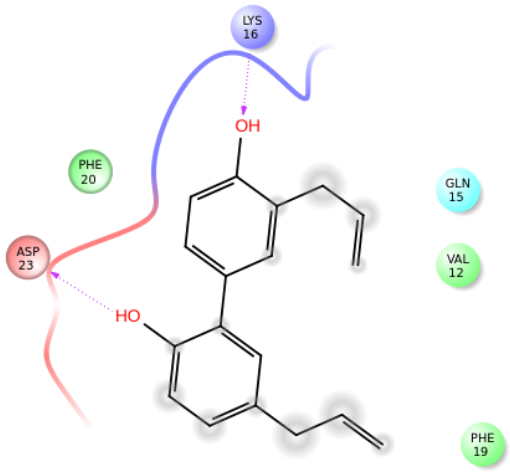

Figure S3. Proposed interactions of honokiol with $A\beta_{42}$ monomer (PDB ID: 1IYT; 2D interactions diagram). Binding interactions: H-bonding (pink arrow) with Lys16 and Asp23.

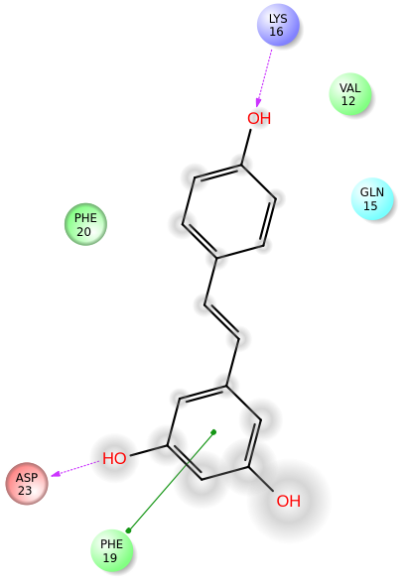

Figure S4. Proposed interactions of resveratrol with $A\beta_{42}$ monomer (PDB ID: 1IYT; 2D interactions diagram). Binding interactions: H-bonding (pink arrow) with Lys16 and Asp23, and π-π interactions (green line) with Phe19.

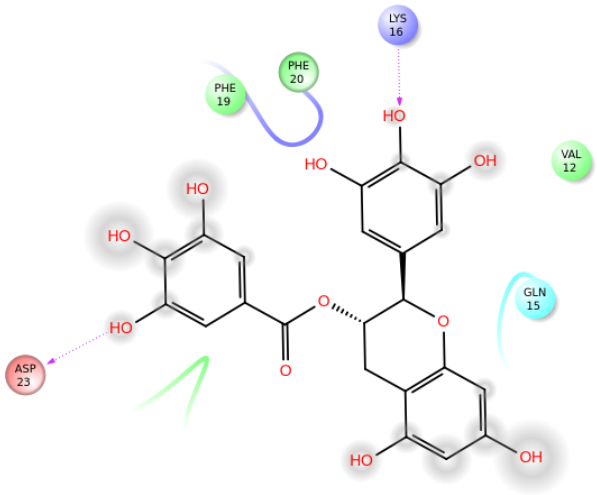

Figure S5. Proposed interactions of EGCG with $A\beta_{42}$ monomer (PDB ID: 1IYT; 2D interactions diagram). Binding interactions: H-bonding (pink arrow) with Lys16 and Asp23.

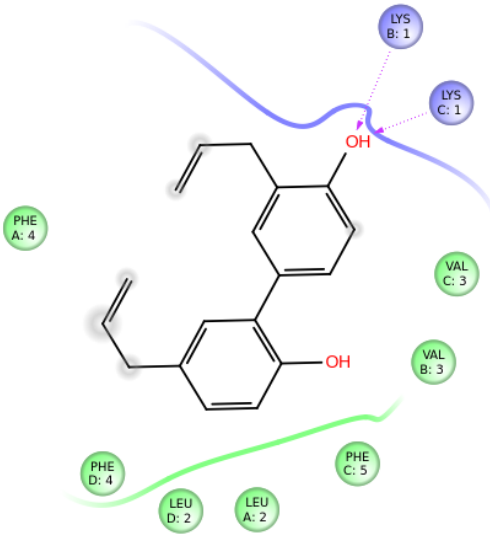

Figure S6. Proposed interactions of honokiol with $A\beta_{16\text{-}21}$ (KLVFFA) fiber (PDB ID: 3OVJ; 2D interactions diagram). Binding interactions: H-bonding (pink arrow) with two Lys16 residues.

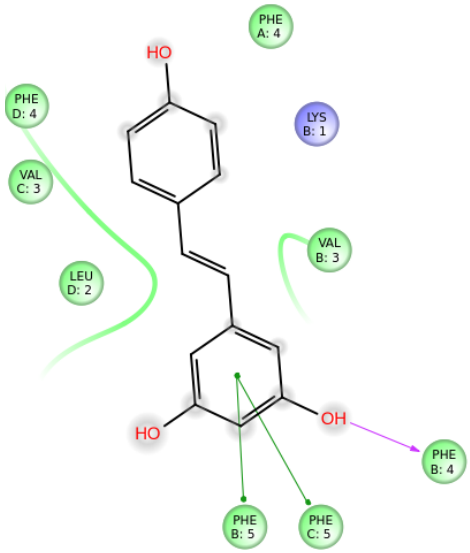

Figure S7. Proposed interactions of resveratrol with $A\beta_{16-21}$ (KLVFFA) fiber (PDB ID: 3OVJ; 2D interactions diagram). Binding interactions: H-bonding (pink arrow) with the amide backbone of Phe19, and π-π stacking (green line) with two Phe20 residues.

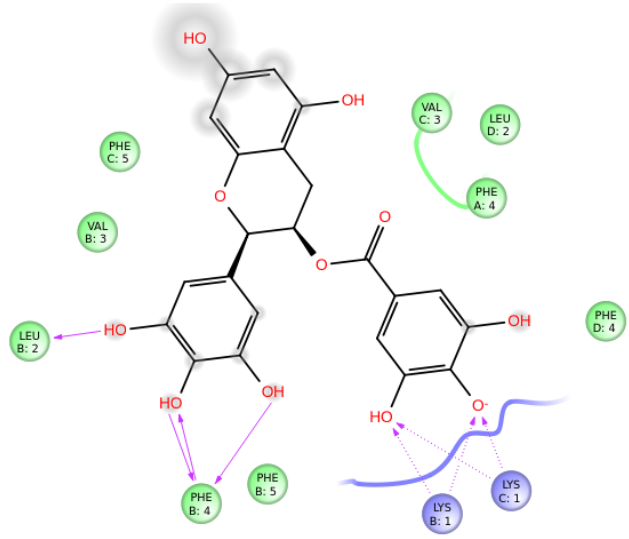

Figure S8. Proposed interactions of EGCG with $A\beta_{16-21}$ (KLVFFA) fiber (PDB ID: 3OVJ; 2D interactions diagram). Binding interactions: H-bonding (pink arrow) with Lys16, Leu17 and Phe19.

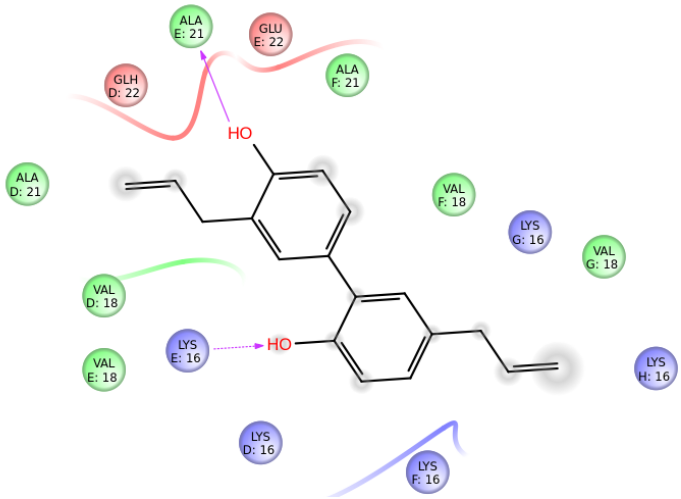

Figure S9. Proposed interactions of honokiol with monomorphic $A\beta_{42}$ amyloid fibrils (PDB ID: 5KK3; 2D interactions diagram). Binding interactions: H-bonding (pink arrow) with Lys16 and Ala21.

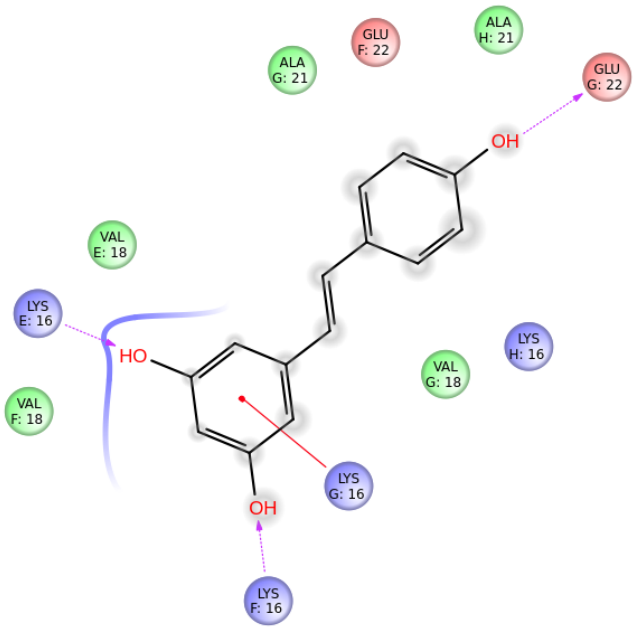

Figure S10. Proposed interactions of resveratrol with monomorphic $A\beta_{42}$ amyloid fibrils (PDB ID: 5KK3; 2D interactions diagram). Binding interactions: H-bonding (pink arrow) with Glu22 and two Lys16 residues, and also made a π-cation (red line) interaction with Lys16.

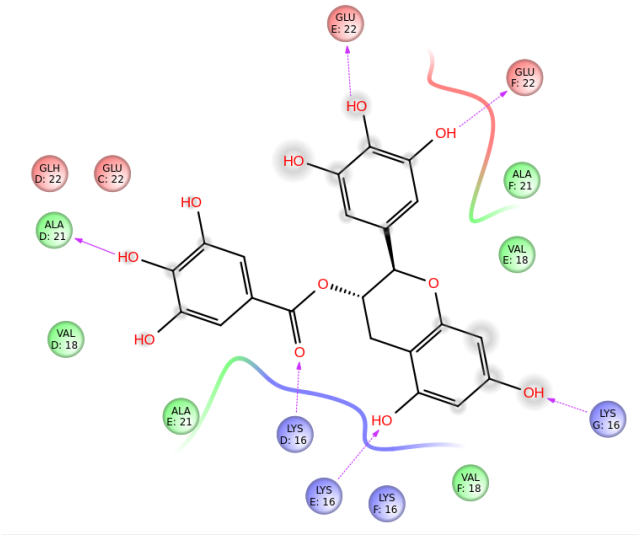

Figure S11. Proposed interactions of EGCG with monomorphic $A\beta_{42}$ amyloid fibrils (PDB ID: 5KK3; 2D interactions diagram). Binding interactions: H-bonding (pink arrow) with Lys16, Ala21 and Glu22.

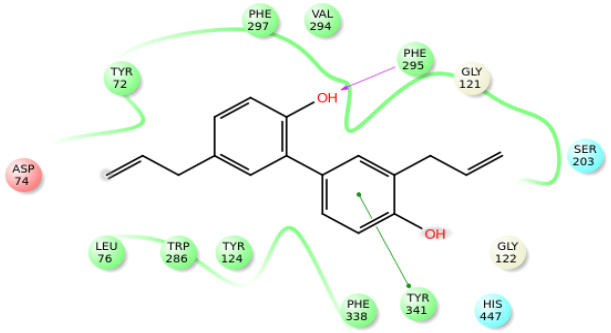

Figure S12. Proposed interactions of honokiol at the binding site of hAChE (PDB ID: 4EY7; 2D interactions diagram). Binding interactions: H-bonding (pink arrow) with the amide backbone of Phe295 and π-π interactions (green line) with Tyr341.

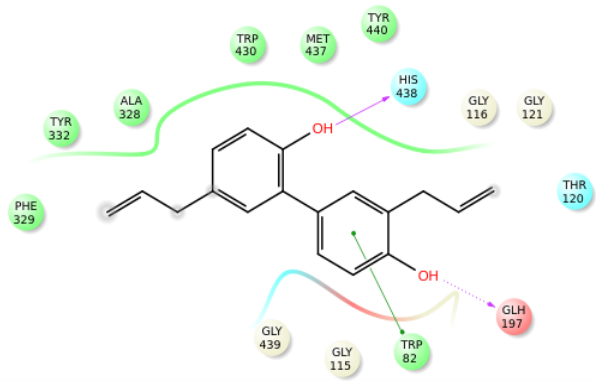

Figure S13. Proposed interactions of honokiol at the binding site of hBuChE (PDB ID: 4TPK; 2D interactions diagram). Binding interactions: H-bonding (pink arrow) with Glh197, the amide backbone of His438 and π-π interactions (green line) with Trp82.

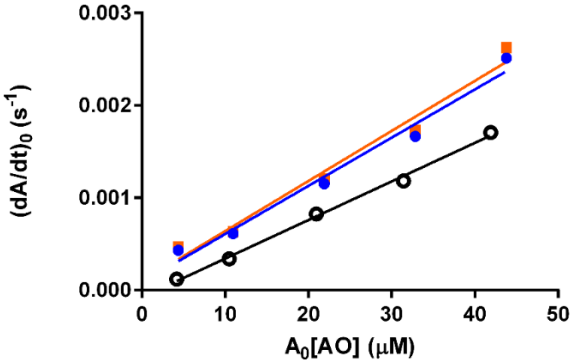

Figure S14. Antioxidant kinetics. Example linear plots of $(dA/dt)_0$ (bleaching rate at time = 0) against $A_0[AO]$ for honokiol ($r^2 \geq 0.9765$). A_0 is the absorbance at time = 0, and [AO] is the concentration of antioxidant at time = 0 in μM.

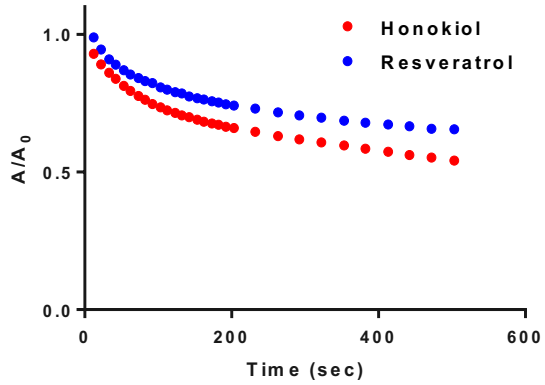

Figure S15. Representative absorbance-time plots of the bleaching of DPPH by honokiol and resveratrol in methanol. The concentration of antioxidants was 25 μM and the concentration of DPPH was 60 μM. A is the absorbance of the sample and A_0 is the absorbance of 60 μM DPPH at 515 nm.

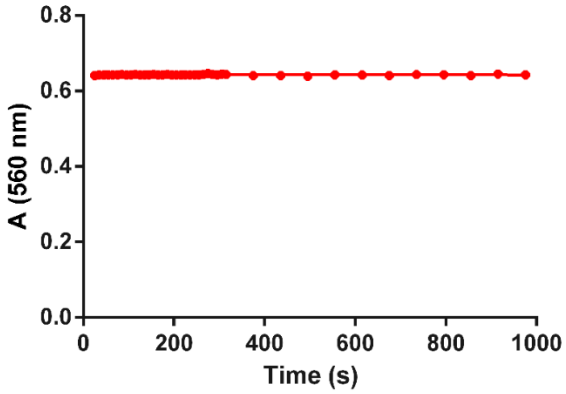

Figure S16. The rapid reaction of ferrozine with Fe(II) in the absence of test compound. Solutions of Fe(II) (25 μM) and ferrozine (1 mM) in HEPES buffer (15 mM, pH 6.8) were mixed and the absorbance at 560 nm was recorded as soon as possible. The absorbance was constant over the time period 25 to 976 s.

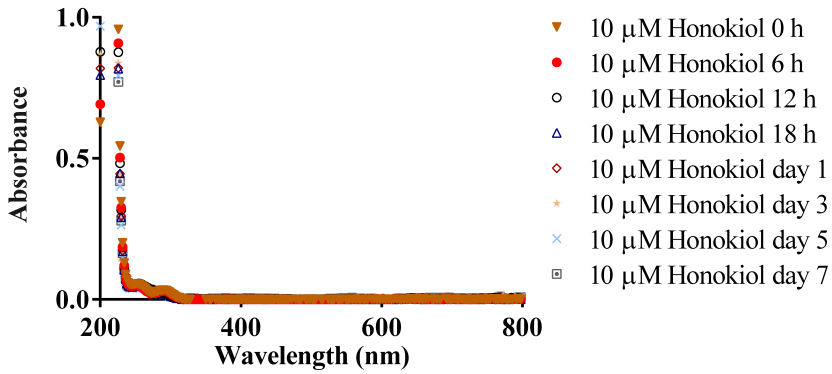

Figure S17. Absorbance spectra of 10 µM honokiol over 7 days. Honokiol (10 µM) was incubated in phosphate buffer (20 mM, pH 7.4, *I* 0.17 M) at 37˚C.

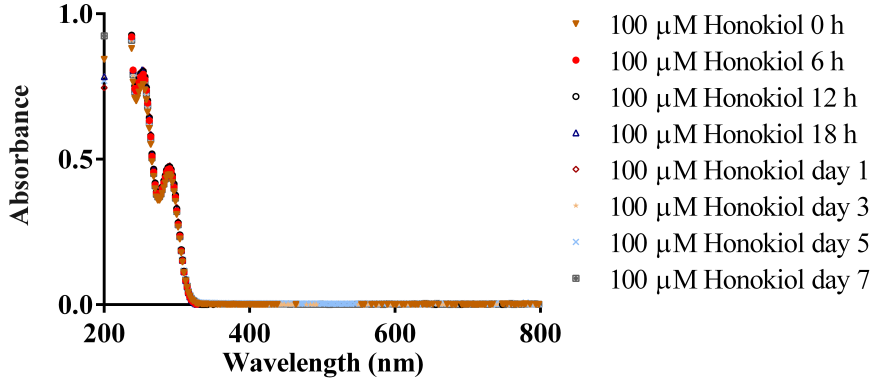

Figure S18. Absorbance spectra of 100 µM honokiol over 7 days. Honokiol (100 µM) was incubated in phosphate buffer (20 mM, pH 7.4, *I* 0.17 M) at 37˚C.

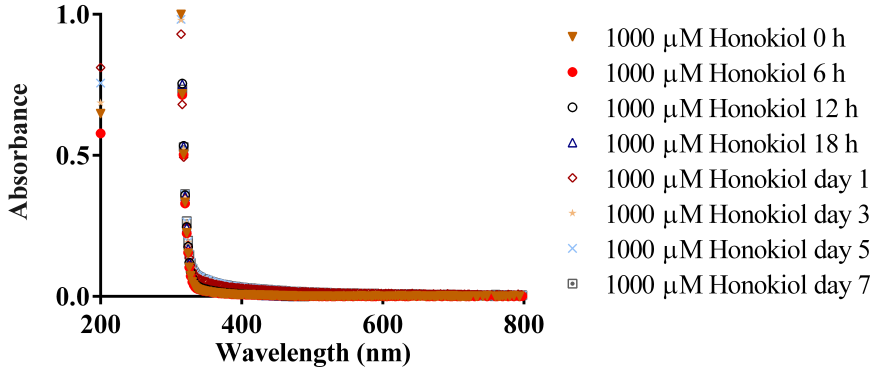

Figure S19. Absorbance spectra of 1000 µM honokiol over 7 days. Honokiol (1000 µM) was incubated in phosphate buffer (20 mM, pH 7.4, *I* 0.17 M) at 37˚C.

Table S1. Iron(II) chelation activities of honokiol and reference compounds estimated using the ferrozine assay.[a]

Compound	Concentration (μM) for 50% chelation of 25 μM iron(II)
Honokiol	535.0 ± 13.0
Resveratrol	746.0 ± 14.1
EGCG	4.7 ± 0.2 [1]
EDTA	10.2 ± 0.1

[a]The phenols resveratrol and EGCG were included for comparison with honokiol. EDTA, which is known to have strong iron(II) chelating ability,[1, 2] was included as a positive control reference compound.

Table S2. Physicochemical properties of honokiol, resveratrol and EGCG predicted *in silico* by Asteris (version 1.1) (www.asteris-app.com).

Properties	**Honokiol**	**Resveratrol**	**EGCG**
2C9 pKi	5.44 (medium)	4.43 (low)	5.56 (medium)
2D6 affinity category	Medium	Medium	Low
Aromatic ring count	2.00	2.00	3.00
BBB category	+	-	-
BBB log([brain]:[blood])	-0.22	-0.21	-0.51
Flexibility	0.24	0.11	0.11
HIA category	+	+	-
H- bond acceptors	2.00	3.00	11.00
H- bond donors	2.00	3.00	8.00
Molecular weight (g/mol)	266.34	228.24	458.37
P-gp category	No	No	No
PAINS count	0.00	0.00	0.00
PPB90 category	High	Low	Low
Rotatable bonds	5.00	2.00	4.00
Topological polar surface area ($Å^2$)	40.46	60.69	197.37
hERG pIC50	5.36	4.84	4.58
log(VDss)	-0.24	-0.53	-0.76
logD	4.36	2.11	1.67
logP	4.36	2.11	1.67
logS	2.26	3.49	2.80
logS @ pH7.4	2.26	3.49	2.80

Table S3: Description of the RP-HPLC analytical method

RP-HPLC conditions	Time (min)	Solvent B (%)
RP-HPLC column: Agilent ZORBAX SB-C18 column with 4.6 × 250 mm, particle size 5 µm, and pore size 80 Å. Gradient elution: Solvent A: 0.1% v/v formic acid in water Solvent B: 0.1% v/v formic acid in acetonitrile Flow rate: 1 mL/min PDA detection at 280 nm	0	10
	10	10
	25	100
	35	100
	40	10
	45	10

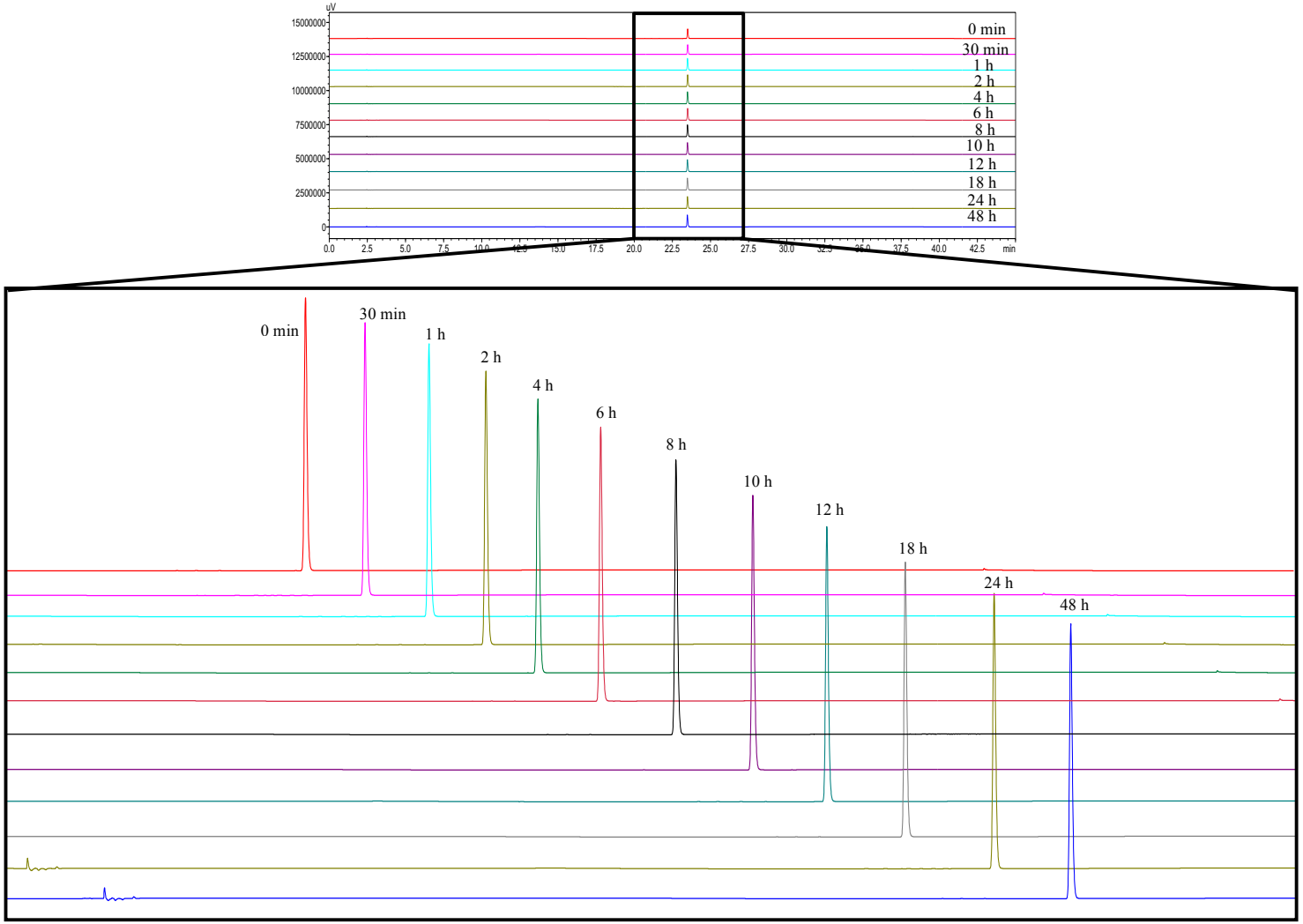

Figure S20. RP-HPLC chromatograms of 100 µM of honokiol incubated over 48 h in phosphate buffer (20 mM, pH 7.4, *I* 0.17 M) at 37°C under quiescent conditions with samples collected at various time points.

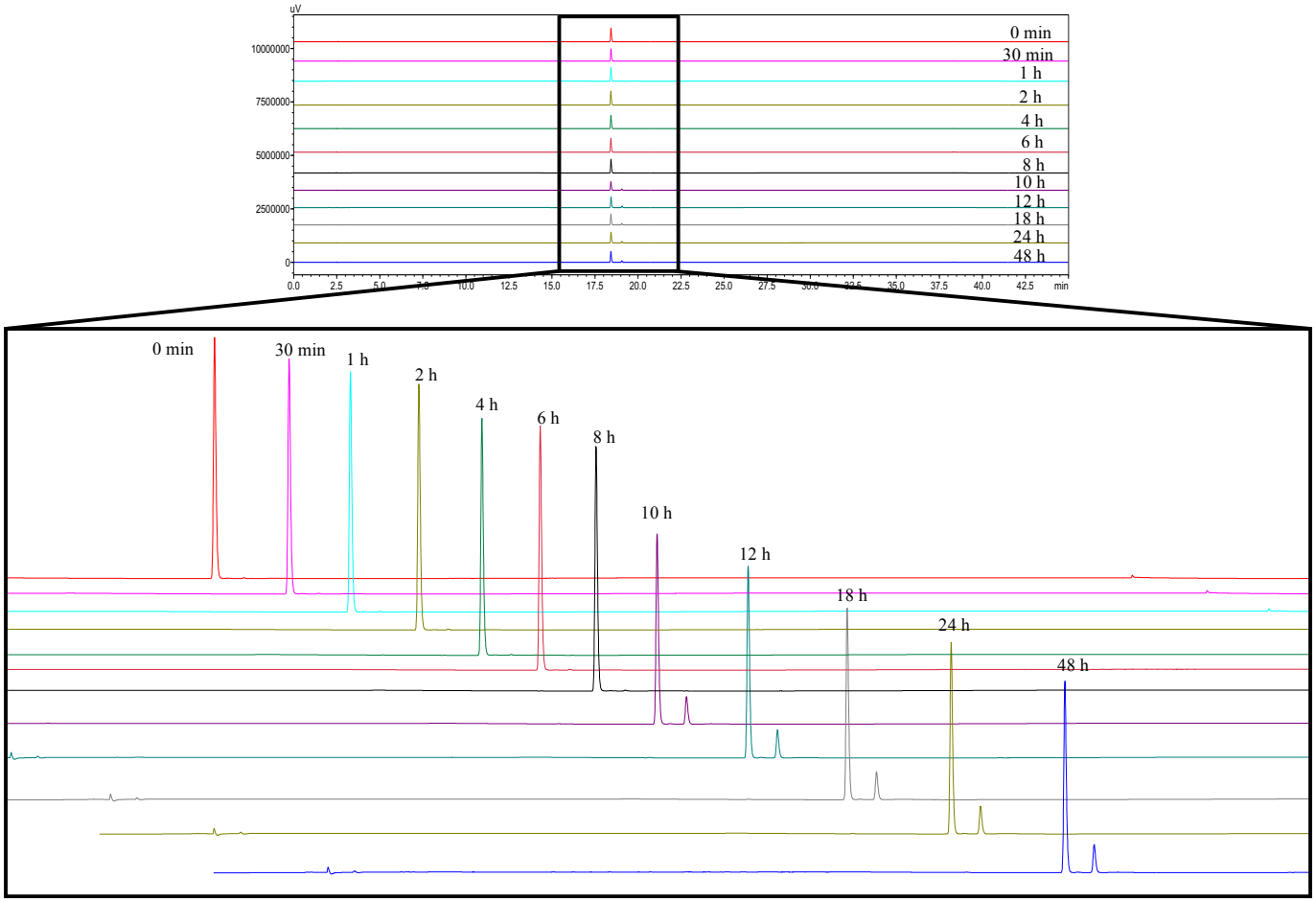

Figure S21. RP-HPLC chromatograms of 100 µM of resveratrol incubated over 48 h in phosphate buffer (20 mM, pH 7.4, *I* 0.17 M) at 37°C under quiescent conditions with samples collected at various time points.

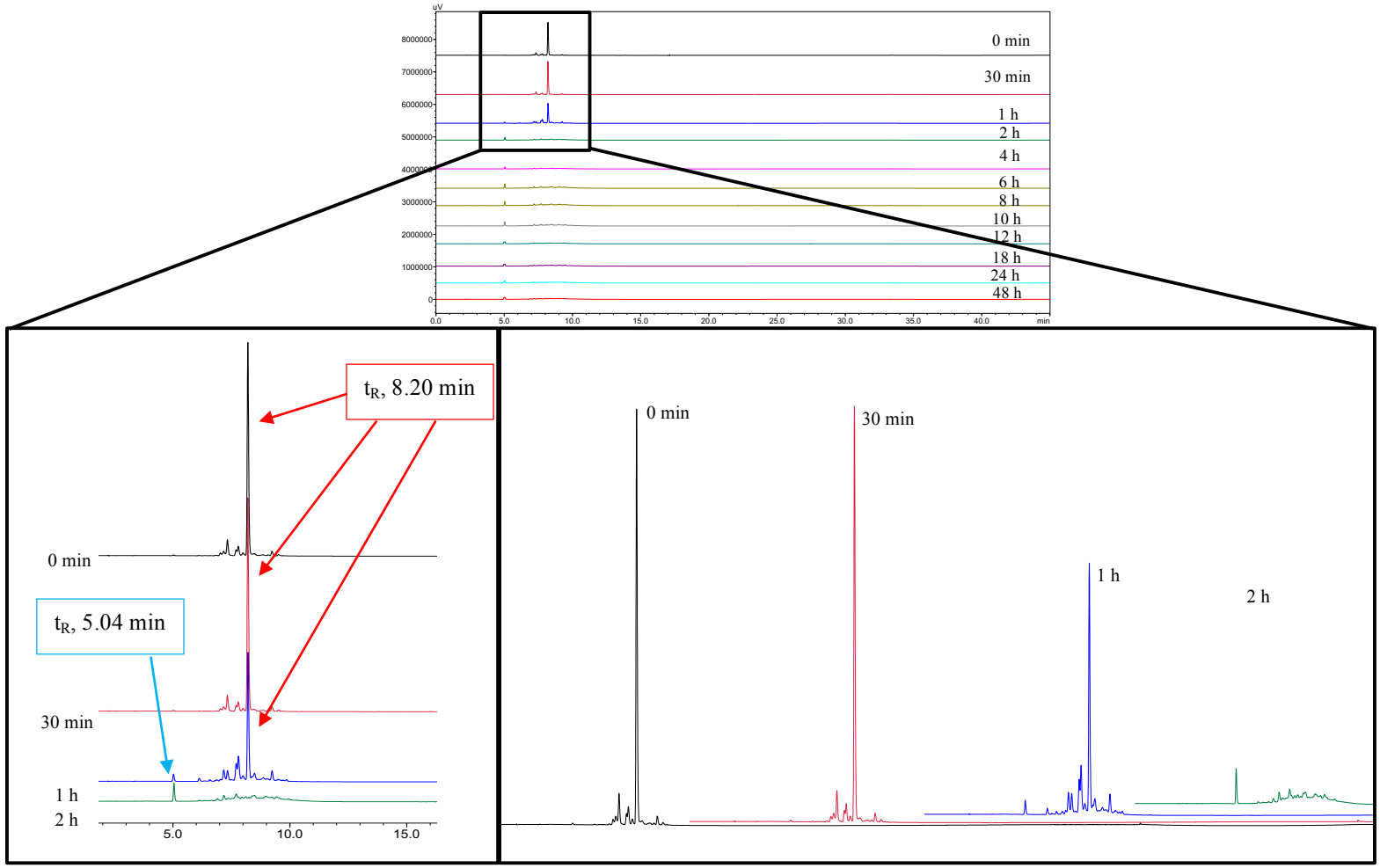

Figure S22. RP-HPLC chromatograms of 100 µM of EGCG incubated over 48 h in phosphate buffer (20 mM, pH 7.4, *I* 0.17 M) at 37°C under quiescent conditions with samples collected at various time points.

The following list of dot points is provided to acknowledge the work of others that could not be cited in the references list due to editorial restrictions.

- Prevelance of Alzheimer's disease.[3]
- Redox potential of iron and copper, and generation of reactive oxygen species via Fenton chemistry.[4]
- Schrödinger molecular modelling suite.[5, 6]
- RCSB Protein Data Bank (PDB; www.rcsb.org).[7]
- Drug-like properties.[8]
- Lead-like properties.[9]
- Ellman's assay.[10, 11]
- Ferrozine assay.[12]
- DPPH assay.[13]
- Auto-oxidation of polyphenols and their toxicity.[14-18]

Supplementary references

(1) Chan, S., Kantham, S., Rao, V. M., Palanivelu, M. K., Pham, H. L., Shaw, P. N., McGeary, R. P., and Ross, B. P. (2016) Metal chelation, radical scavenging and inhibition of Aβ 42-fibrillation by food constituents in relation to Alzheimer's disease, *Food Chem. 199*, 185-194.

(2) Furia, T. E. (1972) Sequestrants in Food, In *CRC Handbook of Food Additives* (Furia, T. E., Ed.) 2nd ed., pp 271-294, CRC Press, Cleveland.

(3) Prince, M., Guerchet, M., and Prina, M. (2013) Policy Brief for Heads of Government: The Global Impact of Dementia 2013–2050, Alzheimer's Disease International, London.

(4) Greenough, M. A., Camakaris, J., and Bush, A. I. (2013) Metal dyshomeostasis and oxidative stress in Alzheimer's disease, *Neurochem. Int. 62*, 540-555.

(5) Schrödinger Release 2014-1 (2014), Maestro, version 9.8, 2014, *Schrödinger, LLC, New York, NY*.

(6) Friesner, R. A., Murphy, R. B., Repasky, M. P., Frye, L. L., Greenwood, J. R., Halgren, T. A., Sanschagrin, P. C., and Mainz, D. T. (2006) Extra precision glide: Docking and scoring incorporating a model of hydrophobic enclosure for protein−ligand complexes, *J. Med. Chem. 49*, 6177-6196.

(7) Berman, H. M., Westbrook, J., Feng, Z., Gilliland, G., Bhat, T. N., Weissig, H., Shindyalov, I. N., and Bourne, P. E. (2000) The protein data bank, *Nucleic Acids Res. 28*, 235-242.

(8) Ghose, A. K., Viswanadhan, V. N., and Wendoloski, J. J. (1999) A knowledge-based approach in designing combinatorial or medicinal chemistry libraries for drug discovery. 1. A qualitative and quantitative characterization of known drug databases, *ACS. Comb. Sci. 1*, 55-68.

(9) Rees, D. C., Congreve, M., Murray, C. W., and Carr, R. (2004) Fragment-based lead discovery, *Nat. Rev. Drug Discov. 3*, 660-672.
(10) Ellman, G. L., Courtney, K. D., Andres, V., and Featherstone, R. M. (1961) A new and rapid colorimetric determination of acetylcholinesterase activity, *Biochem. Pharmacol. 7*, 88-95.
(11) Ingkaninan, K., De Best, C., Van Der Heijden, R., Hofte, A., Karabatak, B., Irth, H., Tjaden, U., Van der Greef, J., and Verpoorte, R. (2000) High-performance liquid chromatography with on-line coupled UV, mass spectrometric and biochemical detection for identification of acetylcholinesterase inhibitors from natural products, *J. Chromatogr. A 872*, 61-73.
(12) Carter, P. (1971) Spectrophotometric determination of serum iron at the submicrogram level with a new reagent (ferrozine), *Anal. Biochem. 40*, 450-458.
(13) Campos, A., Duran, N., Lopez-Alarcon, C., and Lissi, E. (2012) Kinetic and stoichiometric evaluation of free radicals scavengers activities based on diphenyl-picryl hydrazyyl (DPPH) consumption, *J. Chil. Chem. Soc. 57*, 1381-1384.
(14) Bolton, J. L., Trush, M. A., Penning, T. M., Dryhurst, G., and Monks, T. J. (2000) Role of quinones in toxicology, *Chem. Res. Toxicol. 13*, 135-160.
(15) Bae, M. J., Ishii, T., Minoda, K., Kawada, Y., Ichikawa, T., Mori, T., Kamihira, M., and Nakayama, T. (2009) Albumin stabilizes (–)-epigallocatechin gallate in human serum: Binding capacity and antioxidant property, *Mol. Nutr. Food Res. 53*, 709-715.
(16) Flueraru, M., Chichirau, A., Chepelev, L. L., Willmore, W. G., Durst, T., Charron, M., Barclay, L., and Wright, J. S. (2005) Cytotoxicity and cytoprotective activity in naphthalenediols depends on their tendency to form naphthoquinones, *Free Radic. Biol. Med. 39*, 1368-1377.
(17) Mazzanti, G., Menniti-Ippolito, F., Moro, P. A., Cassetti, F., Raschetti, R., Santuccio, C., and Mastrangelo, S. (2009) Hepatotoxicity from green tea: a review of the literature and two unpublished cases, *Eur. J. Clin. Pharmacol. 65*, 331-341.
(18) Tanaka, T. (2008) Chemical studies on plant polyphenols and formation of black tea polyphenols, *Yakugaku Zasshi 128*, 1119-1131.